

PHYTOCHROME C regulation of photoperiodic flowering via *PHOTOPERIOD1* is mediated by *EARLY FLOWERING 3* in *Brachypodium distachyon*

Daniel P. Woods , Weiya Li , Richard Sibout, Mingqin Shao, Debbie Laudencia-Chingcuanco, John P. Vogel, Jorge Dubcovsky, Richard M. Amasino

Published: May 10, 2023 • <https://doi.org/10.1371/journal.pgen.1010706>

⚠ Expression of Concern

Following the publication of this article [1], concerns were raised regarding results presented in Fig 2. Specifically, corresponding author informed PLOS that the underlying expression data reported in this study have been inappropriately manipulated.

The University of California, Davis confirmed that author DPW admitted to manipulation of the data underlying the results presented in Fig 2.

The authors are working with PLOS to try and address these issues. Meanwhile, the *PLOS Genetics* Editors issued an Expression of Concern to notify readers of the above issues.

19 Sep 2023: The PLOS Genetics Editors (2023) Expression of Concern: PHYTOCHROME C regulation of photoperiodic flowering via *PHOTOPERIOD1* is mediated by *EARLY FLOWERING 3* in *Brachypodium distachyon*. *PLOS Genetics* 18(5): e1010955. <https://doi.org/10.1371/journal.pgen.1010955> | [View expression of concern](#)

Abstract

Daylength sensing in many plants is critical for coordinating the timing of flowering with the appropriate season. Temperate adapted grasses such as *Brachypodium distachyon* flower during the spring when days are becoming longer. The phytochrome C is essential for long-day (LD) flowering in *B. distachyon*. *PHYC* is required for the LD activation of genes in the photoperiod pathway including *PHOTOPERIOD1* (*PPD1*) that, in turn, result in the activation of *FLOWERING LOCUS T* (*FT1*)/*FLORIGEN*, which causes flowering. Thus, *B. distachyon phyC* mutants are extremely delayed in flowering. We show that *PHYC*-mediated activation of *PPD1* occurs via *EARLY FLOWERING 3* (*ELF3*), a component of the evening complex of the circadian clock. The extreme delay of flowering of the *phyC* mutant disappears when combined with an *elf3* loss-of-function mutation. Moreover, the dampened *PPD1* expression in *phyC* mutant plants is elevated in *phyC/elf3* mutant plants compared to the rapid flowering of the double mutant. We show that loss of *PPD1* function also results in reduced *FT1* expression, which causes delayed flowering consistent with results from wheat and barley. Additionally, *elf3* mutant plants have elevated expression of *PPD1*, and we show that overexpression of *ELF3* results in delayed flowering associated with a reduction of *PPD1* expression. We show that *ELF3* expression is repressed by *PPD1* transcription consistent with previous studies showing that *ELF3* binds to the *PPD1* promoter. Indeed, *PPD1* is the main target of *ELF3*-mediated flowering as *elf3/ppd1* double mutant plants are not able to flower. Our results indicate that *ELF3* operates downstream from *PHYC* and acts as a repressor of *PPD1* in the photoperiodic flowering pathway of *B. distachyon*.

Author summary

Daylength is an important environmental cue that plants and animals use to coordinate important life history events with the season. In plants, timing of flowering to a particular season is an essential adaptation to many ecological niches. Perceived changes in daylength starts with the perception of light via specific photoreceptors such as phytochromes. In temperate grasses, how daylength perception is integrated into downstream pathways to trigger flowering is not fully understood. However, in

components involved in the translation of daylength perception into the induction of flowering in temperate grasses have been identified from studies of natural variation. For example, specific alleles of two genes called *EARLY FLOWERING 3* (*ELF3*) and *PHOTOPERIOD1* (*PPD1*) have been selected during breeding of different wheat and barley varieties to modulate the flowering response to maximize reproduction in different environments. Here, we show in the temperate grass model *Brachypodium distachyon* that the translation of the light signal perceived by phytochromes into a flowering response is mediated by *PPD1*, and that *PPD1* is genetically downstream of *ELF3* in the photoperiodic flowering pathway. These results provide a genetic basis for understanding the photoperiodic response in temperate grasses that include agronomically important crops such as wheat, barley, and rye.

Citation: Woods DP, Li W, Sibout R, Shao M, Laudencia-Chingcuanco D, Vogel JP, et al. (2023) PHOTOREGULATION OF PHOTOPERIODIC FLOWERING VIA *PHOTOPERIOD1* IS MEDIATED BY *EARLY FLOWERING 3* IN *Brachypodium distachyon*. *PLoS Genet* 19(5): e1010706. <https://doi.org/10.1371/journal.pgen.1010706>

Editor: Claudia Köhler, Max Planck Institute of Molecular Plant Physiology: Max-Planck-Institut für molekulare Pflanzenphysiologie, GERMANY

Received: October 13, 2022; **Accepted:** March 17, 2023; **Published:** May 10, 2023

This is an open access article, free of all copyright, and may be freely reproduced, distributed, transmitted, modified, adapted, and built upon, or otherwise used by anyone for any lawful purpose. The work is made available under the [Creative Commons Public Domain Dedication](#).

Data Availability: All mutant lines are available upon request to the following email address: front_desk@biochem.wisc.edu (Department of Biochemistry, University of Wisconsin) with no restrictions.

Funding: This work was funded in part by the US National Science Foundation (Award IOS-1755224 to RMA) and the Great Lakes Bioenergy Research Center, US Department of Energy, Office of Science, Office of Biological and Environmental Research (Award No. DE-SC0018409). The work from JPV, RS, and MS (proposal: 10.46936/10.25585/6000104) was conducted by the U.S. Department of Energy Joint Genome Institute (<https://ror.org/04xm1d337>), a DOE Office of Science User Facility, is supported by the Office of Science of the U.S. Department of Energy operated under Contract No. DE-AC02-05CH11231. DPW was a Howard Hughes Medical Institute (HHMI) Fellow of the Life Sciences Research Foundation, which supported the work while in Jorge Dubcovsky's lab and paid his salary. JD was funded by HHMI. DLC is funded by the USDA-ARS CRIS Project 2030-21430-014D. The funders had no role in study design, data collection and analysis, decision to publish, or preparation of the manuscript.

Competing interests: The authors have declared that no competing interests exist.

Introduction

The transition from vegetative growth to flowering is an important developmental decision for which the timing is often influenced by the environment (e.g. [1–4]). This critical life history trait has been shaped over evolutionary time to ensure reproduction to coincide with the time of year that is most favorable for flower and seed development. Moreover, breeding the timing of flowering in crops has been critical for adapting various crop varieties to changing environments and to climate (e.g. [5]).

In many plant species, changes in day-length and/or temperature provide seasonal cues that result in flowering during the appropriate time of year [1,6]. Many temperate grasses such as *Brachypodium distachyon* (*B. distachyon*), wheat, and barley that flower in the spring or early summer months in response to increasing day-lengths are referred to as long-day (LD) plants [7]. *B. distachyon* is closely related to the core pooid clade comprising wheat, oats, barley, and rye and has a number of attributes that make it an attractive grass model organism suitable for developmental genetics research [8,9].

Variation in the LD promotion of flowering in temperate grasses such as wheat and barley can be due to allelic variation in *PHOTOPERIOD1* (*PPD1*), a member of the pseudo-response regulator (PRR) gene family (*PPD1* is also known as *PHOTOPERIODIC FLOWERING 1* (*PHF1*) and *PHOTOPERIODIC RESPONSE REGULATOR 37* (*PRR37*)) [10,11]. Natural variation in *PPD1* resulting in either hypomorphic alleles as found in tetraploid wheat or dominant *PPD1* alleles as found in hexaploid wheat impacts flowering [10–15]. Specifically, natural regulatory mutations in the conserved CONSTANS, CONSTANS-LIKE and TIMING OF CAB EXPRESSION 1 (CCT) putative DNA-binding domain in the barley *PPD1* protein cause photoperiod insensitivity and delayed flowering under LD [11, 12], whereas dominant

photoperiod insensitivity is linked to overlapping large deletions in the promoter region of *PPD1* in either the A [13] or homeologs [10]. These deletions result in elevated expression of *PPD1*, particularly during dawn, causing rapid flowering under non-inductive SD conditions [13]. It is worth noting that although these wheat lines are referred to as photoperiod (PI) varieties they still flower earlier under LD than under SD if the timing of flowering is measured as the emergence of spike (heading time) [16]. It has been hypothesized that the large deletion within the *PPD1* promoter might remove a one or more transcriptional repressors [13]. To date, natural variation studies of flowering in *B. distachyon* have not found variation at *PPD1* and thus its role in LD flowering in *B. distachyon* is not known [17–21].

Variation in *EARLY FLOWERING 3* (*ELF3*; also known as *mat* and *eam*) impacts photoperiodic flowering in grasses [22,23], wheat [22,23], barley [24,25], and rice [26]. In these plants, natural variation in *ELF3* allows growth at latitudes that would not be inductive for flowering, enabling these crops to be grown in regions with short growing seasons [5]. For example, *ELF3* maturity (*eam*) loci have been used by breeders to allow barley to grow at higher latitudes in regions of northern Europe with short growing seasons [24,27]. The *eam8* mutant in the barley ortholog of *ELF3*, is a loss-of-function mutation that accelerates flowering under SD or LDs [24,25] similar to *elf3* loss-of-function alleles described previously in the eudicot model *Arabidopsis thaliana* [28]. Moreover, loss of function of *ELF3* in *B. distachyon* also results in rapid flowering under SD and LD, and the *B. distachyon* *ELF3* protein is able to rescue the *A. thaliana* *elf3* mutant, demonstrating a conserved role of *ELF3* across angiosperm diversification [29–31].

Work in *A. thaliana* has shown that *ELF3* is an important component of the circadian clock that acts as a bridge protein in a trimeric protein complex that also contains *LUX ARRTHYHMO* (LUX), and *EARLY FLOWERING 4* (*ELF4*) and is referred to as the evening complex (EC) [32]. Loss-of-function mutations in any of the proteins that make up the EC results in disrupted flowering and rapid flowering [33–36]. The peak expression of the EC at dusk is involved in the direct transcriptional repression of genes that make up the morning loop of the circadian clock including *A. thaliana* *PRR7* and *PRR9*, which are paralogs of grass *PRR73* [37–39]. Recently, it has been shown that the EC also directly represses *PRR37*, *PRR95*, and *PRR73* in rice [40]. The rice ortholog of *PPD1*, *CO1*, has elevated *PPD1* expression [23,24,30] indicating *ELF3* may impact flowering in *B. distachyon* mutants in barley, wheat, and *B. distachyon* have elevated *PPD1* expression [23,24,30] indicating *ELF3* may impact flowering in *B. distachyon* part via *PPD1*, but to what extent remains to be determined.

The photoperiod and circadian pathways converge in the transcriptional activation of florigen/*FLOWERING LOCUS T* in leaves [6,41]. In temperate grasses, *PPD1* is required for the LD induction of *FT1*, whereas in *A. thaliana* *CONSTANS* is the main photoperiodic gene required for *FT1* activation in LD [16,42,43]. There are two *CO*-like genes in temperate grasses. Interestingly, in the presence of functional *PPD1*, *co1co2* wheat plants have a modest earlier heading phenotype suggesting *CO1* and *CO2* are in fact mild floral repressors, but in the absence of *PPD1*, *CO1* acts as a flowering promoter under LD [16]. To date, *co1co2* double mutants have been reported in *B. distachyon*. However, RNAi knock-down of *co1* results in a 30-day delay in flowering under 16h LD [44] and overexpression of *CO1* leads to earlier flowering in SD [44]. These results indicate that *CO1* in *B. distachyon* has a promoting role in flowering even in the presence of a functional *PPD1* gene, and suggest potential differences in the role of *CO1* in the regulation of flowering between *B. distachyon* and wheat.

Once *FT1* is activated by LD it interacts with the bZIP transcription factor *FD* which triggers the expression of the MADS box transcription factor *VERNALIZATION1* (*VRN1*) [45,46]. *VRN1* in turn upregulates the expression of *FT1* forming a positive feedback loop that overcomes the repression from the zinc finger and CCT domain-containing transcription factor *VERNALIZATION2* (*VRN2*) [17,47–50]. The *FT1* protein is then thought to migrate from the leaves to the shoot apical meristem, as shown in *A. thaliana* [51,52], to induce the expression of floral homeotic genes including *VRN1*, thus converting the vegetative meristem into a reproductive meristem under favorable LD photoperiods.

Light signals are perceived initially by photoreceptors that initiate a signal transduction cascade impacting a variety of developmental responses to light [53]. The sensing of light is accomplished by complementary photoreceptors: phytochromes that perceive the ratio of red and far-red light, cryptochromes, phototropins, and Zeiltlupe family proteins that detect blue light, and UV-B RESISTANCE LOCUS 8 that detects ultraviolet B light [54,55]. The phytochromes form homodimers that upon exposure to red light undergo a conformation shift to an active form causing the activation of a suite of downstream genes [54]. Conversely, exposure of plants to far-red or dark conditions causes reversion of the phytochromes to an inactive state [54].

There are three phytochromes in temperate grasses referred to as *PHYTOCHROME A* (*PHYA*), *PHYTOCHROME B* (*PHYB*) and *PHYTOCHROME C* (*PHYC*) [56]. Functional analyses of these phytochromes in temperate grasses revealed that *PHYA* and *PHYB* play a major role in the LD induction of flowering because loss-of-function mutations in either of these genes results in delayed flowering [57–59] whereas loss-of-function mutations in *PHYA* in *B. distachyon* results in only a modest delay in flowering under inductive LD, indicating *PHYB* and *PHYC* are the main light receptors required for photoperiodic flowering in temperate grasses [29]. The important role of *PHYC* in photoperiodic flowering is not universal as loss of *phyC* function in *A. thaliana* results in

only has small effects on flowering [60,61].

In temperate grasses, PHYB and PHYC are required for the transcriptional activation of a suite of genes involved in the photoperiodic flowering pathway, including *PPD1*, *CO1*, and *FT1*, and ectopic expression of *FT1* in the *B. distachyon* *phyC* background results in a reversal of the *phyC* single-mutant, delayed-flowering phenotype [57,58,62]. Moreover, consistent with the beginning of the photoperiodic flowering signal cascade, expression of genes encoding components of the circadian clock are also severely dampened in the *phyB* and *phyC* mutant backgrounds [29,57–59]. An exception to this is that the expression of *ELF3* is not altered in the temperate grass phytochrome mutants [29,58,59]. Recently, in *B. distachyon* it has been shown that PHYC can interact with ELF3, and this interaction destabilizes the ELF3 protein indicating that the regulation of ELF3 is at least in part at the protein level consistent with previous studies from *A. thaliana*, rice, and the companion study in wheat [23,29,40,63–66]. At present it is not clear to what extent the regulation of ELF3 by PHYs is critical for photoperiodic flowering.

Here, we show in *B. distachyon* by analyzing *phyC/elf3* double mutant plants that indeed the light signal perceived by the phytochromes is mediated through ELF3 for photoperiodic flowering. The extreme delayed flowering of the *phyC* mutant in the *phyC/elf3* double mutant which flower as rapidly as the *elf3* single mutant. Moreover, the expression profiles of genes in the photoperiod pathway are similar between *elf3* and *phyC/elf3* mutants compared to *phyC* mutants. Thus, *elf3* is complementary to *phyC* at the phenotypic and molecular levels. Furthermore, we show strong, environment-dependent genetic interactions between *ELF3* and *PPD1*, which indicates that *PPD1* is a main target of ELF3-mediated repression of flowering. These results provide a genetic and molecular framework to understand photoperiodic flowering in the temperate grasses.

Results

Rapid flowering of *elf3* is epistatic to the delayed flowering of *phyC*

Previous studies in *B. distachyon* showed that PHYC can affect the stability of the ELF3 protein, and that the transcriptional profile of the *phyC* mutant resembles that of a plant with elevated ELF3 signaling [29]. Thus, it has been suggested that the extreme delayed flowering phenotype of the *phyC* mutant [58] could be mediated by ELF3 [29]. To test the extent to which the translational signal perceived by PHYC to control flowering is mediated by ELF3, we generated *elf3/phyC* double mutant plants and compared the flowering of the double mutant relative to that of *elf3* and *phyC* single mutants as well as Bd21-3 wild type under 16h-SD and 8h-SD (Fig 1).

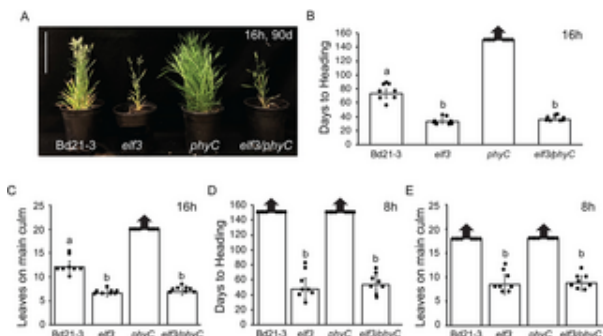


Fig 1.

The rapid flowering of the *elf3* mutant is epistatic to the delayed flowering of the *phyC* mutant (A) Representative plants of Bd21-3 wild-type, *elf3*, *phyC* and *elf3/phyC* double mutant plants grown in a 16h photoperiod at 90d after germination. Plants are 17cm. (B, D) Flowering times under 16h (B) or 8h daylengths (D) measured as days to heading of Bd21-3, *elf3*, *phyC*, and *elf3/phyC*. (C) Flowering phenotypes under 16h (C) or 8h daylengths (E) measured as the number of leaves on the main culm at time of heading. Bars represent the average of 8 plants \pm SD. Arrows above bars indicate that none of the plants flowered at the end of the experiment (150d). Letters (a, b) indicate statistical differences ($p < 0.05$) according to the HSD test used to perform multiple comparisons.

<https://doi.org/10.1371/journal.pgen.1010706.g001>

Under both 16h LD and 8h SD photoperiods, we found that *elf3* is epistatic to *phyC*. Specifically, in LD *elf3/phyC* double mutants flowered rapidly by 38 days with 6.9 leaves similar to *elf3* mutants that flowered by 34 days with 6.6 leaves (Fig 1A and 1B). In contrast, *phyC* mutants had not flowered after 150 days with greater than 20 leaves when the experiment was terminated. Bd21-3 wild-type flowered by 72 days with 12 leaves consistent with previous studies [49,58]. In 8h SD, *elf3/phyC* double mutants flowered rapidly by 38 days with 6.9 leaves similar to *elf3* mutants that flowered by 34 days with 6.6 leaves (Fig 1A and 1B). In contrast, *phyC* mutants had not flowered after 150 days with greater than 20 leaves when the experiment was terminated. Bd21-3 wild-type flowered by 72 days with 12 leaves consistent with previous studies [49,58].

also flowered rapidly by 54 days with 8.8 leaves similar to *elf3* mutants that flowered by 48 days with 8.5 leaves (Fig 1D). In contrast, both Bd21-3 wild-type and *phyC* mutants had not flowered by 150 days with >18 leaves when the experiment was terminated (Fig 1D and 1E). These results indicate that the extreme delayed flowering mutant phenotype of *phyC* in wheat is mediated by *ELF3*.

To determine if *PHYC* affects the expression of *ELF3*, we analyzed *ELF3* mRNA levels across a diurnal light cycle (0-24h dark). There were no significant differences in *ELF3* expression at any time point in the *phyC* mutant relative to wild-type, indicating that *PHYC* does not affect the transcriptional profile of *ELF3* in *B. distachyon* consistent with results from wheat (67, 69).

Effect of mutations in *PHYC* and *ELF3* on the transcriptional profiles of flowering time genes

To further understand how *PHYC* and *ELF3* affect flowering at a molecular level, we compared the mRNA levels of *ELF3* and orthologs of the photoperiod and vernalization pathway genes *FT1*, *VRN1*, *PPD1*, *VRN2*, *CO1*, and *CO2* across a diurnal cycle in 16h LD in the *phyC* and *elf3* single mutants versus the *elf3/phyC* double mutant (Fig 2). We were particularly interested in determining how the expression profiles of “flowering-time genes” in the *elf3/phyC* double mutant compared to the *elf3* single mutant. The newly expanded fourth leaf was harvested for gene expression analyses because at this developmental stage in 16h daylengths the meristems of all of the plant genotypes are at a vegetative stage and thus are developmentally equivalent. Consistent with the rapid flowering of the *elf3* and *elf3/phyC* mutants, the mRNA expression levels of *FT1* and *VRN1* in these mutants are significantly higher than the levels in wild-type and *phyC* mutants across all the time points tested (Fig 2A and 2B). In contrast, the overall expression profiles of *FT1* and *VRN1* in the *elf3* and *elf3/phyC* mutants were similar throughout the day, in contrast to the *phyC* mutant in which *FT1* and *VRN1* mRNA levels were lower than wild type throughout the day compared to the delayed flowering phenotype of *phyC*. Although the elevated levels of *FT1* and *VRN1* in both *elf3* and *elf3/phyC* are consistent with their rapid flowering, the expression of the floral repressor, *VRN2*, exhibits a similar elevated expression profile throughout the day in both *elf3* and *elf3/phyC* relative to wild-type or *phyC* single-mutants (Fig 2E). The elevated *VRN2* expression levels in these plants are consistent with previous results in *B. distachyon* and other grasses [23,29,30,40,64]. The transcriptional profile of *CO1* was similar in both the *elf3* and *elf3/phyC* mutants with elevated expression compared to wild-type between zt4-8 and lower than wild-type between zt12-20 (Fig 2C). A similar expression pattern was found for *Hd1* (the rice *CO* homolog) in the *elf3/phyC* double mutant in rice [40]. Consistent with previous reports, *CO1* expression levels remained low in *Brachypodium* throughout a diurnal cycle [58]. By contrast *CO1* expression is increased in the *phyC* mutants in wheat [57] indicating a difference in the regulation of *CO1* between these two species. Lastly, the *CO2* expression profiles were similar between *elf3*, *elf3/phyC*, and *phyC*, whereas *CO2* mRNA levels were lower in *phyC* throughout a diurnal cycle (Fig 2F). In summary, the transcriptional profiles of *FT1*, *VRN1*, *VRN2*, *CO1*, and *CO2* are similar between *elf3* and *elf3/phyC* mutants consistent with *ELF3* acting downstream from *PHYC* in the photoperiod flowering pathway.

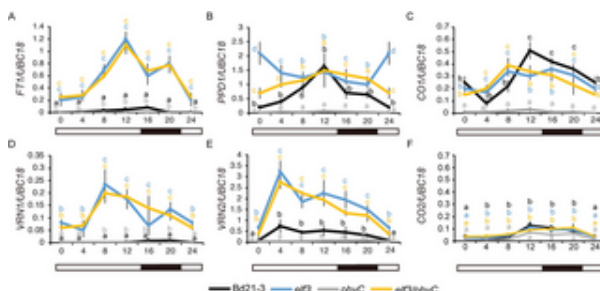


Fig 2. Effect of loss-of-function mutations in *ELF3* and *PHYC* on the transcriptional profiles of six flowering time genes in 16h LD. Normalized expression of (A) *FT1*, (B) *PPD1*, (C) *CO1*, (D) *VRN1*, (E) *VRN2*, and (F) *CO2* during a 24h diurnal cycle. Bd21-3 (black line), *elf3* (blue line), *phyC* (gray line) and *elf3/phyC* double mutant (orange line). Plants were grown until the fourth-leaf stage was reached (Zadoks = 14) at which point the newly expanded fourth leaf was harvested at zt0, zt4, zt8, zt12, zt16, and zt20. Note the zt0 value and zt24 value are the same. The average of four biological replicates (three leaves per replicate). Error bars represent standard deviation of the mean. Data were normalized using *UBP1* as reference gene and done in [49].

<https://doi.org/10.1371/journal.pgen.1010706.g002>

The transcriptional profile of *PPD1* indicates a more complex interaction between *PHYC* and *ELF3*. In wild type, the expression levels of *PPD1* peak at zt12 with the lowest expression level at dawn and during the evening consistent with previous results [65].

PPD1 expression patterns in *B. distachyon* [29,30] (Fig 2B). In both the *elf3* and *elf3/phyC* mutants, we observed increased expression relative to wild-type at dawn and during the evening with expression levels similar to wild-type at zt12. In contrast, increased expression of *PPD1* observed at dawn and during the night in the *elf3/phyC* background was significantly higher than that of the *elf3* single mutant suggesting *PHYC* may impact *PPD1* expression via additional genes beyond *ELF3*. In contrast, expression levels were reduced in the *phyC* mutant relative to wild type, *elf3*, and *elf3/phyC* mutants throughout a diurnal cycle, consistent with the reduced *FT1* expression and delayed flowering phenotype of the *phyC* mutant.

Identification and mapping of a *ppd1* mutant in *B. distachyon*

To determine the role of *PPD1* in flowering in *B. distachyon*, the genome-sequenced, sodium-azide mutant line NaN610 was obtained. A predicted high-effect mutation impacting a splice acceptor donor site in *PPD1* (BdiBd21-3.1G0218200) was obtained from the JGI (<https://phytozome-next.jgi.doe.gov/jbrowse/>). A quarter of the NaN610 M3 seeds re-segregating for an extremely delayed flowering phenotype (Fig 3B–3D).

Due to the high mutant load of these NaN mutant lines, we validated through mapping that the delayed flowering phenotype associated with *PPD1* (Fig 3E and 3F). We backcrossed NaN610 with Bd21-3 and confirmed a quarter of the plants in the population ($n = 380$) were delayed flowering, demonstrating the recessive nature of the mutant. Three Derived Cleaved Polymorphic Sequences (dCAPs) markers closely linked with *PPD1* were developed based on the variant's information from the NaN610 line, with one of the dCAPs primers located within the *PPD1* locus itself (Fig 3E and S1 Table). This approach allowed us to map the causative lesion to within a 1 Mb interval (13.1 Mb-14.2 Mb) on the top arm of chromosome 1, demonstrating that the flowering phenotype is tightly linked with *PPD1* (Fig 3E).

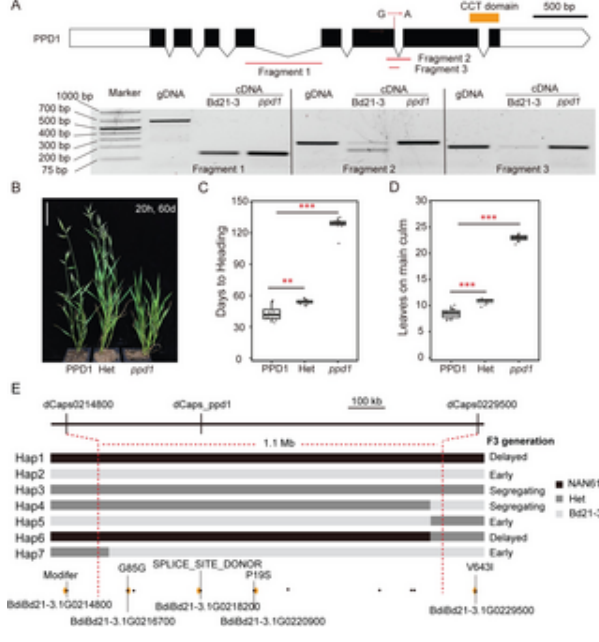


Fig 3. Identification of a *ppd1* mutant.

(A) Gene structure of *PPD1* showing the location of the nucleotide change of the sodium azide-induced mutation indicates the region that encodes the CCT domain. Below the gene structure diagram is a gel image of the reverse transcription polymerase chain reaction (PCR) (30 cycles of amplification) showing PCR products of *PPD1* cDNA and *ppd1* mutant plants. The location of primers used in each reaction are shown in the diagram above the gel image. Representative photo of Bd21-3, heterozygous, and homozygous *ppd1* plants grown in a 20h LD. Picture was taken after germination in 20h LD, bar = 5cm. **(C and D)** Flowering time was measured as days to heading (**C**) and the number of spikelets on the parent culm at time of heading (**D**), ** indicates statistical differences ($p < 0.01$), *** indicates statistical differences ($p < 0.001$) by Student's t-test. **(E)** Fine mapping of *ppd1* in a population of 380 BC1F2 individuals. Individuals with seven different haplotypes were identified by three dCAPS markers and flowering times of each haplotype were determined in the F2 generation. Black, grey, and light grey rectangles represent NAN610, heterozygous, and Bd21-3 genotypes, respectively. Variants around the *PPD1* locus from the NAN610 line are shown with black dots, and yellow arrows indicate the genes within the mapped interval with the specific effect on the coding region indicated.

<https://doi.org/10.1371/journal.pgen.1010706.g003>

To confirm that the predicted splice site mutation does in fact impact the splicing of *PPD1*, we sequenced the mRNA of *ppd1* NaN610 mutant line and Bd21-3 (Fig 3A). We found that the splice site mutation resulted in the mis-splicing of generating a reading frame shift resulting in a truncated protein lacking the conserved CCT domain (Fig 3A). The extended flowering of the *B. distachyon* *ppd1* mutant is consistent with the *ppd1* null mutants described in wheat, which takes 10-15 days to head under inductive LD conditions [16,43], demonstrating *PPD1* is required for LD flowering broadly within grasses.

Genetic interactions between *ELF3* and *PPD1* under long and short days

We and others have shown that *PPD1/PRR37* expression is increased in an *elf3* mutant background in *B. distachyon* wheat (Fig 2B; [29,30,40,66]). Moreover, a ChIPseq analysis of *ELF3* demonstrated that *PPD1* is directly bound by day-night-responsive manner [29,40]. Thus, *ELF3* acts as a direct transcriptional repressor of *PPD1* but the extent to which this explains the rapid flowering in the *elf3* mutant has not been tested. Therefore, we generated an *elf3/ppd1* double mutant to test the genetic interactions of these two genes under a highly inductive 20h LD, inductive 16h LD, and non-inductive 8h SD.

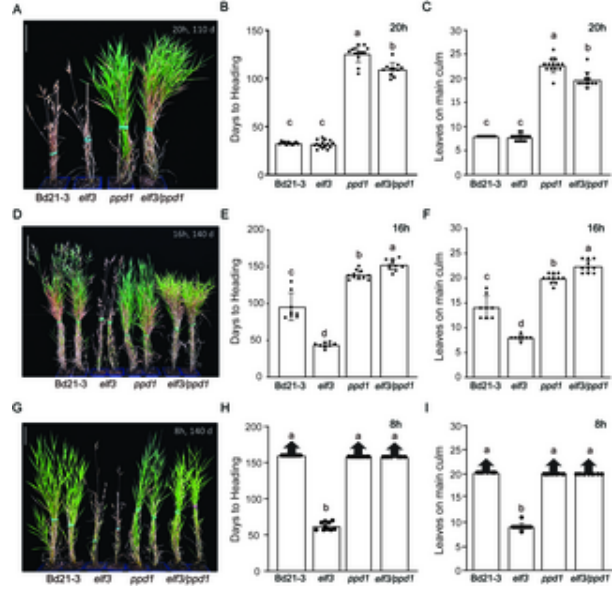


Fig 4. Genetic interactions between the delayed flowering *ppd1* mutant and the rapid flowering *elf3* mutant.

Representative image of Bd21-3 wild-type, rapid flowering *elf3* mutant, delayed flowering *ppd1* mutant, and delayed *elf3/ppd1* double mutant grown in a 20h photoperiod (A), 16h photoperiod (D), and 8h photoperiod (G). Picture was taken after 110d, for the 20h LD (A) and 140d after germination for the 16h LD and (D) 8h SD. Scale bar = 5cm. (B, E, H) Days to heading times under 20h (B), 16h (E), 8h (G) measured as days to heading of Bd21-3, *elf3*, *ppd1*, and *elf3/ppd1*. Flowering under 20h (C), 16h (F), and 8h (I) measured as the number of leaves on the parent culm at time of heading. The experiment was repeated three times. The first experiment resulted in *ppd1* plants that stopped producing new leaves after 110d, similar to wild type. One possibility for the cessation of new leaf production in *ppd1* plants in this experiment is that the meristem transitioned to flowering, but then did not proceed to heading. However, in two subsequent experiments *ppd1* plants continued to produce new leaves for the duration of the experiment similar to wild type and this data is shown in (C, F, I). All three experiments are shown in S1 Data for Fig 4. When grown under non-inductive conditions for 120 days of 8h SD, *B. distachyon* plants flower; we consider this a stochastic flowering response because the majority of plants do not flower. Bars represent the average of 8 plants \pm SD. Arrows above bars indicate that none of the plants flowered at the end of the experiment (150d, >20 leaves). Letters (a, b, c, d) indicate statistical differences ($p < 0.05$) according to a Tukey's HSD test used to perform multiple comparisons.

<https://doi.org/10.1371/journal.pgen.1010706.g004>

Under all photoperiods, the *elf3/ppd1* double mutant flowered significantly later than the *elf3* single mutant (Fig 4). In 20h LD, the *elf3/ppd1* double mutant flowered earlier than *ppd1* by 16.2 days forming 3.0 fewer leaves where as in 8h SD, *elf3/ppd1* mutant flowered significantly later than *ppd1* by 13.7 days with 2.5 more leaves. In 8h SD, only *elf3* plants were able to flower; Bd21-3, *ppd1*, and *elf3/ppd1* all failed to flower by the end of the experiment. It is also worth noting that *elf3/ppd1* double mutants are still able to respond to different photoperiods, with longer days resulting in significantly earlier flowering plants than under shorter days (Fig 4B and 4E and 4H). These results indicate that there are strong genetic interactions between *ELF3* and *PPD1*.

between *ELF3* and *PPD1* under different photoperiods, that *PPD1* is a key flowering regulator downstream of *ELF3*, is a residual photoperiodic response that is independent of these two genes.

Effect of mutations in *ELF3* and *PPD1* on the transcriptional profiles of flowering time genes

To understand how *ELF3* and *PPD1* affect flowering at a molecular level, we measured the mRNA levels of *FT1*, *VRN2*, *CO1*, and *CO2* in the *elf3* and *ppd1* single mutants and the *elf3/ppd1* double mutant across a diurnal cycle in 16h LD. As noted before, *FT1* and *VRN1* expression levels were elevated in the *elf3* mutant background; however, in the *elf3/ppd1* mutant, expression of these genes remained low and resembled the expression profile of *ppd1* single mutants (Fig 5A–5E). The low expression levels of *FT1* and *VRN1* in *ppd1* and *ppd1/elf3* mutants is consistent with the delayed flowering phenotype of these mutants in 16h LD. The *VRN2* expression profile was similar between wild type and *ppd1* mutant plants with increased expression levels at dawn and increased expression throughout the light cycle before expression levels dropped in the evening (Fig 5E). Interestingly, *VRN2* expression levels are similarly elevated throughout the day in *elf3* and *elf3/ppd1* mutants compared to wild type (Fig 5E).

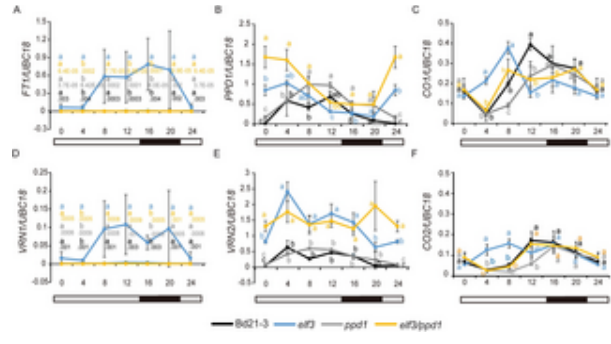


Fig 5. Effect of loss-of-function mutations in *ELF3* and *PPD1* on the transcriptional profiles of six flowering-time genes in 16h LD. The fourth newly expanded leaves were harvested every 4h over a 24-hour period; three biological replicates (two replicates) were harvested at each time point for each genotype. Diurnal expression of *FT1* (A), *PPD1* (B), *CO1* (C), *VRN2* (E), and *CO2* (F) were detected in *Bd21-3* (black line), *elf3* (blue line), *ppd1* (grey line) and *elf3/ppd1* double mutant (orange line). Bars represent the average of three biological replicates \pm SD. Letters (a, b, c, d) indicate statistical differences ($P < 0.05$) according to a Tukey's HSD test used to perform multiple comparisons, letter color corresponds to the four genotypes. The black, gray, and orange lines overlap given the scale used to show *ELF3* expression in the same line. The orange line is arbitrarily shown on top. Specific expression values are shown below the lettered statistical test. Raw data included in S1 Data file.

<https://doi.org/10.1371/journal.pgen.1010706.g005>

Consistent with the expression patterns of *PPD1* in wild type and *elf3* shown in Fig 2, the expression levels of *PPD1* in wild-type and the *elf3* mutant has increased *PPD1* expression relative to wild type at dawn and during the evening (Fig 5B). The expression levels in the *ppd1* mutant should be interpreted with caution because we do not know the effect of the specific mutation on the mRNA stability. Significantly higher levels of *PPD1* expression were observed in *ppd1* relative to wild type at ZT4, ZT8, ZT12, and ZT16, and in *elf3/ppd1* relative to *elf3* at dawn. However, the expression patterns of *PPD1* were most similar between wild type and between *elf3/ppd1* and *elf3* (Fig 5B).

CO1 and *CO2* expression both exhibit peak expression in wild type at zt12 with expression dampening in the evening, consistent with previous reports [29,58]. Interestingly, expression levels of *CO1* and *CO2* were elevated between zt4-8 in *elf3* compared to wild-type. However, at zt16 and zt20, expression levels were similar in wild type, *elf3*, and *elf3/ppd1* mutants, whereas expression of *CO1* was reduced in *elf3* compared to wild type. In contrast, the expression levels of *CO1* and *CO2* were higher in *ppd1* compared to the other lines at zt8. In the *elf3/ppd1* mutants, *CO1* and *CO2* expression was most similar to *ppd1* in the morning and most similar to *elf3* in the evening (Fig 5C and 5F). These results indicate complex interactions between *ELF3* in the regulation of *CO1* and *CO2*.

Constitutive expression of *ELF3* results in delayed flowering and lower *PPD1*, *FT1*, and *VRN1* expression levels

In our previous study, we showed that overexpression of *ELF3* in the *elf3* mutant background results in strongly delayed flowering ([30], Fig 6A). However, this was done in the T0 generation, so we evaluated the flowering time and expression of *ELF3*

flowering-time genes in the T1 generation. We grew four *UBI::ELF3/elf3* transgenic lines alongside Bd21-3 and *elf3* mutant compared with wild-type [29,30]; Figs 2 and 5). We first confirmed that all of the *UBI::ELF3/elf3* transgenic lines elevated *ELF3* mRNA levels, and found indeed there is a significant increase of *ELF3* expression in the transgenic lines. To understand how *UBI::ELF3/elf3* affects flowering, we evaluated expression levels of *FT1*, *VRN1*, *PPD1*, *VRN2*, *CO1*, and *CO2* in wild type, *elf3*, and *UBI::ELF3/elf3*. Consistent with the delayed flowering, *FT1* and *VRN1* expression levels of *UBI::ELF3/elf3* were reduced relative to wildtype compared to elevated levels *elf3* relative to wildtype (Fig 6D and 6G). Also, the expression levels of *VRN2*, *CO1*, and *CO2* were decreased in *UBI::ELF3/elf3*, indicating *ELF3* is playing a broad repressive role in regulating domain containing genes responding to photoperiodic flowering.

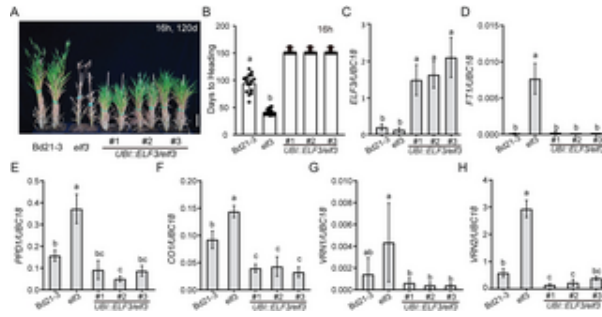


Fig 6. Overexpression of *ELF3* in the *elf3* mutant delays flowering.

(A) Representative image of Bd21-3 wild type, *elf3*, and three independent transgenic lines of *UBI::ELF3* in the *elf3* background grown in a 16h photoperiod. Images were taken 120d after germination. Bar = 5 cm. The fourth newest leaves were harvested at zt4 in 16h. (B-I), Normalized expression of *ELF3* (C), *FT1* (D), *PPD1* (E), *CO1* (F), *VRN1* (G), and *VRN2* (H) in Bd21-3 wild type, *elf3*, and three *UBI::ELF3/elf3* transgenic lines. Expression of *CO2* is shown in S2 Fig. Bars represent the average of four biological replicates \pm SD.

<https://doi.org/10.1371/journal.pgen.1010706.g006>

Discussion

The phytochromes *PHYC/PHYB* and *ELF3* connection

B. distachyon has an obligate requirement for LD to flower [8,49,67]. Previous studies have shown the important role of *PHYC* and *ELF3* play in photoperiodic flowering in *B. distachyon* [29,30,58]. Specifically, mutations in *phyC* result in delayed flowering whereas loss-of-function mutations in *elf3* result in rapid flowering in either LD or SD [30,58]. Further, *phyC* mutants resemble plants grown in SD both morphologically and at the transcriptomic level regardless of day-length [58]. *elf3* mutants resemble plants grown in LD both morphologically and at the transcriptomic level regardless of day-length [29]. Thus, we were interested in exploring the genetic relationships between *PHYC* and *ELF3*. The extreme delayed flowering phenotype observed in *phyC* mutant plants is mediated by *ELF3* because *phyC/elf3* double mutants flower rapidly in a manner similar to *elf3* mutants. Similar genetic interactions between *phyB* and *elf3* were also found in wheat in the companion study, suggesting these interactions are likely to be conserved broadly in temperate grasses. Loss-of-function mutations in *phyB* also result in delayed flowering similar to *phyC* [59]. At present, no null *phyB* alleles have been reported in *B. distachyon*. However, *PHYB* is able to heterodimerize with *PHYC* in *B. distachyon* and wheat [29, 57], and both *phyB* [59] and *phyC* [57] mutants show extremely late flowering in wheat suggesting that both *PHY*s are likely required for photoperiodic flowering in the temperate grasses, perhaps because *PHYB/PHYC* heterodimers are required for flowering regulation.

Phytochrome regulation of *ELF3* at the post-translational level rather than at the transcriptional level is likely to be the primary interaction impacting flowering. In *A. thaliana*, *B. distachyon*, and wheat, *phyB/phyC* mutants do not impact the circadian rhythms of *ELF3* mRNA levels [29,59,68]. However, in all three species *PHYB* and *PHYC* have been shown to interact with the *ELF3* protein, but the stability of the *ELF3* protein upon exposure to light differs between *A. thaliana* and temperate grasses. Specifically, in *A. thaliana*, *PHYB* contributes to the stability of the *ELF3* protein during light exposure leading to ELF3 protein accumulation at the end of the day [63,68], whereas in rice *ELF3* is degraded and or modified during light exposure in a *PHY*-mediated manner [40]. In temperate grasses, *ELF3* protein accumulates during the night and is rapidly degraded or modified upon light exposure [29,67], and this is likely to be a *PHY* mediated response as well.

The differences in how phytochromes impact the stability of the ELF3 protein might explain the contrasting flowering in either LD or SD and *phyC* mutants flower earlier under SD [60], whereas in temperate grasses *phyB* or *phyC* mutants are extremely delayed in flowering [57–59]. However, ELF3 acts as a flowering repressor in both *A. thaliana* and grasses. *A. thaliana* PHYB stabilizes the ELF3 protein; therefore, in *phyB* mutants, ELF3 is no longer stable leading to rapid flowering. In contrast, in temperate grasses and rice, in the absence of *phyB* or *phyC* the ELF3 protein is more stable leading to delayed flowering.

Interestingly, overexpression of ELF3 results in extremely delayed flowering in *B. distachyon* [29,30] (Fig. 6A and 6B). Since regulation of ELF3 appears to occur at the protein level, one might not expect that overexpression would cause such a strong flowering delay. However, if the ELF3 protein is expressed at a high level such that the degradation machinery is unable to process much of the ELF3 protein during LD, then a strong flowering delay might occur. In support of this idea, the delayed flowering caused by overexpression of ELF3 is mitigated when plants are grown under constant light versus 16h LD [29]. It is worth noting that overexpression of ELF3 generally leads to delayed flowering in different plant species, there is considerable variation in the magnitude of this delayed flowering [29,63,66] (Fig. 6A and 6B).

Similar genetic interactions between *ELF3* and *PHYB* have also been observed in rice which is a SD-flowering plant. In rice-specific *ELF3* paralogs [70]. Mutations in either paralog results in delayed flowering in SD or LD in contrast to the early flowering observed in temperate grasses containing *elf3* mutations [40,71,72]. Also in contrast to the situation in temperate grasses, *phyB* mutants flower more rapidly than wild type in rice [73]. Despite the flowering differences of the *elf3* and *phyB* mutants between rice and temperate grasses, the flowering phenotype of *phy* mutants is ELF3 mediated because in both rice and temperate grasses *elf3* is epistatic to *phyB* or *phyC* [Fig. 1; 40, 67]. Moreover, PHYB and ELF3 proteins interact impacting the light modification of ELF3 by light [40]. The opposite roles that phytochromes and *elf3* have on flowering in rice and temperate grasses is likely due, at least in part, to the reverse role that the downstream *PPD1/PRR37* gene has on flowering. *PPD1* is a repressor of flowering in LD temperate grasses but is a repressor of flowering in SD grasses such as rice [11,16,74,75] (Fig. 3).

The *ELF3* and *PPD1* connection

The extremely delayed flowering of *B. distachyon* *ppd1* mutant plants under LD is similar to the extremely delayed flowering mutants in wheat [16]. However, a previous study in *B. distachyon* using a CRISPR induced *ppd1* mutant allele which has a deletion in the sixth exon of *PPD1* has a milder delayed flowering phenotype with plants taking around 40 days to flower under LD, whereas the mutant *ppd1* plants presented here flower around 120 days in 20h LD [29]; Figs 3 and 4). In both species, wild-type Bd21-3 plants flower on average between 25–30 days in 20h LD consistent with previous reports in *B. distachyon*. The differences in flowering time between the two *B. distachyon* *ppd1* mutant alleles suggests that the CRISPR induced *ppd1* allele is a weaker hypomorphic allele than the *ppd1* mutant allele characterized in this study. This is further supported by the fact that the *ppd1* allele described here has an extremely delayed flowering phenotype similar to the null *ppd1* wheat allele [16].

The *ppd1/elf3* double mutant is delayed in flowering relative to *elf3* mutant plants indicating that *PPD1* is downstream of ELF3 in photoperiodic flowering. This is also consistent with the elevated *PPD1* expression levels observed at dawn and dusk in the *ppd1* mutant relative to wild-type in temperate grasses [30,70] (Fig. 5). Indeed, ELF3 binds to the *PPD1/PRR37* promoter in *B. distachyon*, wheat, and rice indicating ELF3 is a direct transcriptional repressor of *PPD1/PRR37* in grasses [29,40,66]. ELF3 does not have any known DNA binding activity and thus, the direct repression is likely to be due to ELF3's interaction with a transcription factor which, from studies in *A. thaliana*, recognizes GATWCG motifs that are also found in the *PPD1* promoter in temperate grasses [37,38,67]. Interestingly, photoperiod insensitivity in wheat is associated with deletions in the *PPD1* promoter that remove the LUX binding site and results in elevated *PPD1* expression at dawn similar to the *PPD1* expression dynamics observed in *elf3* and *lux* mutant plants [10–13,39,77,78]. In the companion wheat paper, ChIP-PCR experiments show ELF3 enrichment in the DNA region around the LUX binding site in the *PPD1* promoter, which is present within the region deleted in photoperiod-insensitive wheats. These results demonstrate that removal of the evening complex binding site leads to elevated expression of *PPD1* and accelerated heading under SD in many photoperiod-insensitive wheats [66].

The characterization of *elf3/ppd1* mutant plants under different photoperiods reveal complex interactions between the two genes and their downstream targets depending on the environment. For example, *elf3/ppd1* mutant plants are earlier flowering than *ppd1* mutant plants under 20h day-lengths, but are later flowering under 16h and 8h day-lengths. This is in contrast to *elf3* mutants in wheat, which head earlier than *ppd1* under a 16h day-lengths indicating that ELF3 can delay heading independently of *PPD1* under this condition [66]. Thus, there are differences between *B. distachyon* and wheat in the effects of ELF3 on heading in the absence of *PPD1*. We speculate that these differences may be related to the different interactions observed between *CO1* and other flowering genes (e.g. *PHY*) in these two species. For example, in wheat *phyC* and *ppd1* mutants, *CO1* expression levels are elevated compared to wild type, whereas in *B. distachyon* *CO1* expression is reduced in both mutants [57,58,66].

Materials and methods

Plant materials and growth conditions

The rapid flowering mutant *elf3* and four *UBI::ELF3/elf3* transgenic lines in *B. distachyon* were previously characterized [58]. All the mutants used for phenotyping and expression in this study were backcrossed at least twice with the wild-type Bd21-3 accession. Seeds were imbibed in the dark at 5°C for three days before planting. Three photoperiods 8h-SD (8h light/16h dark), 16h-LD (16h light/ 8h dark), and 20h-LD (20h light/ 4h dark) were used. For *elf3* plants were grown at the University of California-Davis in growth chambers with metal halide and sodium bulbs as the light source and a temperature of 22°C during light periods and 17°C during dark periods. Light intensity was approximately 300 μmol m-2 s-1 at plant height. For Figs 4 and 5, plants were grown at the University of Wisconsin-Madison in growth chambers with T5 light bulbs (5000 K), and light intensity was approximately 200 μmol m-2 s-1 at plant height. Temperatures averaged 22°C during light periods and 18°C during dark periods. Flowering time was estimated by measuring days to heading and leaves on the plant at the time of heading. Recording of days to heading was done as the days from seed germination to the first emergence of a spike.

Generation of *elf3/phyC* and *elf3/ppd1* double-mutant lines

Epistasis analysis between *phyC*, *ppd1*, and *elf3* was studied by generating *elf3/phyC* and *elf3/ppd1* double mutants. *elf3* was crossed with *phyC* and *elf3/phyC* homozygous double mutant plants were selected in a segregating F2 population by genotyping using primers in [S1 Table](#). Similarly, *ppd1* was crossed with *elf3*, and *elf3/ppd1* homozygous double mutant plants were selected by genotyping using primers in [S1 Table](#) in the segregating F2 population. Flowering time of *elf3/ppd1* double mutants were estimated by growing with Bd21-3, *elf3*, *ppd1* side by side in 8h SD, 16h LD, and 20h LD, and *elf3/phyC* double mutants were grown in 8h SD and 16h LD.

RNA extraction and qPCR

The method for RNA extraction, cDNA synthesis and quantitative PCR (qPCR) is described in [\[49\]](#). Primers used for expression analyses are listed in [S1 Table](#).

Statistical analyses

Comparison of more than two genotypes were performed by using *agricolae* package in R [\[79\]](#). Statistically significant differences among different genotypes were calculated by using one-way analysis of variance (ANOVA) followed by a Tukey's HSD test. Student's t-test was used for analyzing the difference between two genotypes, significant if P< 0.05.

Supporting information

S1 Fig. Effect of loss of function mutations in *PHYC* on the transcriptional profile of *ELF3*.

<https://doi.org/10.1371/journal.pgen.1010706.s001>

(TIF)

S2 Fig. Normalized expression of *CO2* detected in Bd21-3, *elf3*, and three *UBI::ELF3/elf3* transgenic lines.

<https://doi.org/10.1371/journal.pgen.1010706.s002>

(TIF)

S1 Table. Primers used in this study.

<https://doi.org/10.1371/journal.pgen.1010706.s003>

(PDF)

S1 Data. S1_Data.xlsx file contains all raw data used in this study.

<https://doi.org/10.1371/journal.pgen.1010706.s004>

(XLSX)

Acknowledgments

Thanks to Frédéric Bouché for fruitful discussions about photoperiod sensing in *B. distachyon*.

References

1. Andrés F, Coupland G. The genetic basis of flowering responses to seasonal cues. *Nat Rev Genet.* 2012;13: 627–639. pmid:22898651
[View Article](#) • [PubMed/NCBI](#) • [Google Scholar](#)
2. Fjellheim S, Boden S, Trevaskis B. The role of seasonal flowering responses in adaptation of grasses to temperate climates. *Front Plant Sci.* 2018;9: 25221560
[View Article](#) • [PubMed/NCBI](#) • [Google Scholar](#)
3. Bouché F, Woods DP, Amasino RM. Winter Memory throughout the Plant Kingdom: Different Paths to Flowering. *Plant Physiol.* 2017;174: 1135–1146. pmid:27756819
[View Article](#) • [PubMed/NCBI](#) • [Google Scholar](#)
4. Gaudinier A, Blackman BK. Evolutionary processes from the perspective of flowering time diversity. *New Phytol.* 2020;225: 1883–1898. pmid:32403000
[View Article](#) • [PubMed/NCBI](#) • [Google Scholar](#)
5. Bendix C, Marshall CM, Harmon FG. Circadian Clock Genes Universally Control Key Agricultural Traits. *Molecular Plant.* 2015;8: 1135–1146. pmid:25772379
[View Article](#) • [PubMed/NCBI](#) • [Google Scholar](#)
6. Song YH, Shim JS, Kinmonth-Schultz HA, Imaizumi T. Photoperiodic Flowering: Time Measurement Mechanisms in Leaves. *Annu Rev Plant Biol.* 2015;66: 441–464. pmid:25534513
[View Article](#) • [PubMed/NCBI](#) • [Google Scholar](#)
7. Woods DP, Amasino RM. Dissecting the Control of Flowering Time in Grasses Using *Brachypodium distachyon*. *Genetics and Genomics of Brachypodium*. Cham: Springer International Publishing; 2015. pp. 259–273. https://doi.org/10.1007/978-3-319-1510-5_13
8. Raissig MT, Woods DP. The wild grass *Brachypodium distachyon* as a developmental model system. *Curr Top Dev Biol.* 2022; 147:33–56. pmid:35203000
[View Article](#) • [PubMed/NCBI](#) • [Google Scholar](#)
9. Hasterok R, Catalán P, Hazen SP, Roulin AC, Vogel JP, Wang K, et al. Brachypodium: 20 years as a grass biology model system; the way forward. *Trends in Plant Science.* 2022;27: 1002–1016. pmid:35644781
[View Article](#) • [PubMed/NCBI](#) • [Google Scholar](#)
10. Beales J, Turner A, Griffiths S, Snape JW, Laurie DA. A Pseudo-Response Regulator is misexpressed in the photoperiod insensitive *Ppd-H1* allele of wheat (*Triticum aestivum* L.). *Theor Appl Genet.* 2007;115: 721–733. pmid:17634915
[View Article](#) • [PubMed/NCBI](#) • [Google Scholar](#)
11. Turner A, Beales J, Faure S, Dunford RP, Laurie DA. The pseudo-response regulator *Ppd-H1* provides adaptation to photoperiod in barley. *Plant J.* 2005;310: 1031–1034. pmid:16284181
[View Article](#) • [PubMed/NCBI](#) • [Google Scholar](#)
12. Campoli C, Shtaya M, Davis SJ, Korff von M. Expression conservation within the circadian clock of a monocot: natural variation at barley *Ppd-H1* affects circadian expression of flowering time genes, but not clock orthologs. *BMC Plant Biol.* 2012;12: 1–1. pmid:22720803
[View Article](#) • [PubMed/NCBI](#) • [Google Scholar](#)
13. Wilhelm EP, Turner AS, Laurie DA. Photoperiod insensitive *Ppd-A1a* mutations in tetraploid wheat (*Triticum durum* Desf.). *Theor Appl Genet.* 2008;117: 285–294. pmid:18839130
[View Article](#) • [PubMed/NCBI](#) • [Google Scholar](#)
14. Shaw LM, Turner AS, Herry L, Griffiths S, Laurie DA. Mutant Alleles of *Photoperiod-1* in Wheat (*Triticum aestivum* L.) That Confer a Late Flowering Phenotype in Long Days. *PLoS ONE.* 2013;8: e79459. pmid:24244507
[View Article](#) • [PubMed/NCBI](#) • [Google Scholar](#)

15. Seki M, Chono M, Matsunaka H, Fujita M, Oda S, Kubo K, et al. Distribution of photoperiod-insensitive alleles *Ppd-B1a* and *Ppd-D1a* and heading time in Japanese wheat cultivars. *Breed Sci.* 2011;61: 405–412. pmid:23136478
[View Article](#) • [PubMed/NCBI](#) • [Google Scholar](#)

16. Shaw LM, Li C, Woods DP, Alvarez MA, Lin H, Lau MY, et al. Epistatic interactions between PHOTOPERIOD1, CONSTANS1 and CONSTANS-LIKE1 regulate the photoperiodic response in wheat. *PLoS Genet.* 2020;16: e1008812–28. pmid:32658893
[View Article](#) • [PubMed/NCBI](#) • [Google Scholar](#)

17. Woods DP, Bednarek R, Bouché F, Gordon SP, Vogel JP, Garvin DF, et al. Genetic Architecture of Flowering-Time Variation in *Brachypodium*. *Plant Physiol.* 2017;173: 269–279. pmid:27742753
[View Article](#) • [PubMed/NCBI](#) • [Google Scholar](#)

18. Bettgenhaeuser J, Corke FMK, Opanowicz M, Green P, Hernández-Pinzón I, Doonan JH, et al. Natural Variation in *Brachypodium* Link Loci as Major Flowering Determinants. *Plant Physiol.* 2017;173: 256–268. pmid:27650449
[View Article](#) • [PubMed/NCBI](#) • [Google Scholar](#)

19. Gordon SP, Contreras-Moreira B, Woods DP, Marais Des DL, Burgess D, Shu S, et al. Extensive gene content variation in the *Brachypodium* pan-genome correlates with population structure. *Nature Communications.* 2017;8: 1–13. pmid:29259172
[View Article](#) • [PubMed/NCBI](#) • [Google Scholar](#)

20. Tyler L, Lee SJ, Young ND, Delulio GA, Benavente E, Reagon M, et al. Population Structure in the Model Grass *Brachypodium* Is Highly Correlated with Differences across Broad Geographic Areas. *The Plant Genome.* 2016;9: 0–20. pmid:27898828
[View Article](#) • [PubMed/NCBI](#) • [Google Scholar](#)

21. Wilson P, Streich J, Borevitz J. Genomic Diversity and Climate Adaptation in *Brachypodium*. *Genetics and Genomics of *Brachypodium*.* International Publishing; 2015. pp. 107–127.

22. Zikhali M, Wingen LU, Griffiths S. Delimitation of the *Earliness per se D1 (Eps-D1)* flowering gene to a subtelomeric chromosomal deletion in *(Triticum aestivum)*. *Journal of Experimental Botany.* 2015;67: 287–299. pmid:26476691
[View Article](#) • [PubMed/NCBI](#) • [Google Scholar](#)

23. Alvarez MA, Tranquilli G, Lewis S, Kippes N, Dubcovsky J. Genetic and physical mapping of the earliness per se locus *Eps-Am1* in *Triticum* identifies *EARLY FLOWERING 3 (ELF3)* as a candidate gene. *Funct Integr Genomics.* 2016; 1–18. pmid:27085709
[View Article](#) • [PubMed/NCBI](#) • [Google Scholar](#)

24. Faure S, Turner AS, Gruszka D, Christodoulou V, Davis SJ, Korff von M, et al. Mutation at the circadian clock gene *EARLY MATURITY LOCUS* domesticated barley (*Hordeum vulgare*) to short growing seasons. *Proc Natl Acad Sci USA.* 2012;109: 8328–8333. pmid:22566625
[View Article](#) • [PubMed/NCBI](#) • [Google Scholar](#)

25. Zakhrebekova S, Gough SP, Braumann I, Müller AH, Lundqvist J, Ahmann K, et al. Induced mutations in circadian clock regulator *Mat1* for multi-season adaptation and range extension in cultivated barley. *Proc Natl Acad Sci USA.* 2012;109: 4326–4331. pmid:22371569
[View Article](#) • [PubMed/NCBI](#) • [Google Scholar](#)

26. Matsubara K, Ogiso-Tanaka E, Hori K, Ebana K, Ando T, Yano M. Natural variation in *Hd17*, a homolog of *Arabidopsis ELF3* that is involved in photoperiodic flowering. *Plant and Cell Physiology.* 2012;53: 709–716. pmid:22399582
[View Article](#) • [PubMed/NCBI](#) • [Google Scholar](#)

27. Lundqvist U. Eighty years of Scandinavian barley mutation genetics and breeding. In *Induced Plant Mutations in the Genomics Era*, Shukla (Food and Agriculture Organization of the United Nations), 2009 pp. 39–43.

28. Hicks KA, Albertson TM, Wagner DR. *EARLY FLOWERING3* encodes a novel protein that regulates circadian clock function and flower. *Plant Cell*. 2001;13: 1281–1292. pmid:11402160
[View Article](#) • [PubMed/NCBI](#) • [Google Scholar](#)

29. Gao M, Geng F, Klose C, Staudt A-M, Huang H, Nguyen D, et al. Phytochromes measure photoperiod in *Brachypodium*. *bioRxiv*. 2019
[View Article](#) • [Google Scholar](#)

30. Bouché F, Woods DP, Linden J, Li W, Mayer KS, Amasino RM, et al. *EARLY FLOWERING 3* and Photoperiod Sensing in *Brachypodium*. *Plant Sci*. 2021;12: 769194. pmid:35069625
[View Article](#) • [PubMed/NCBI](#) • [Google Scholar](#)

31. Huang H, Gehan MA, Huss SE, Alvarez S, Lizarraga C, Gruebbling EL, et al. Cross-species complementation reveals conserved function of *FLOWERING 3* between monocots and dicots. *Plant Direct*. 2017;1: e00018–14. pmid:31245666
[View Article](#) • [PubMed/NCBI](#) • [Google Scholar](#)

32. Huang H, Nusinow DA. Into the Evening: Complex Interactions in the *Arabidopsis* Circadian Clock. *Trends in Genetics*. 2016;32: 674–682. pmid:27594171
[View Article](#) • [PubMed/NCBI](#) • [Google Scholar](#)

33. Covington MF, Panda S, Liu XL, Strayer CA, Wagner DR, Kay SA. ELF3 modulates resetting of the circadian clock in *Arabidopsis*. *Plant Cell*. 2010;22: 1305–1315. pmid:21402162
[View Article](#) • [PubMed/NCBI](#) • [Google Scholar](#)

34. Nusinow DA, Helfer A, Hamilton EE, King JJ, Imaizumi T, Schultz TF, et al. The ELF4–ELF3–LUX complex links the circadian clock to control of hypocotyl growth. *Nature*. 2011;475: 398–402. pmid:21753751
[View Article](#) • [PubMed/NCBI](#) • [Google Scholar](#)

35. Hazen SP, Schultz TF, Pruneda-Paz JL, Borevitz JO, Ecker JR, Kay SA. *LUX ARRHYTHMO* encodes a Myb domain protein essential for circadian rhythms. *Proc Natl Acad Sci USA*. 2005;102: 10387–10392. pmid:16006522
[View Article](#) • [PubMed/NCBI](#) • [Google Scholar](#)

36. Doyle MR, Davis SJ, Bastow RM, McWatters HG, Kozma-Bognar L, Nagy F, et al. The *ELF4* gene controls circadian rhythms and flowering in *Arabidopsis thaliana*. *Nature*. 2002;419: 74–77. pmid:12214234
[View Article](#) • [PubMed/NCBI](#) • [Google Scholar](#)

37. Silva CS, Nayak A, Lai X, Hutin S, Hugouvieux V, Jung J-H, et al. Molecular mechanisms of Evening Complex activity in *Arabidopsis*. *Proc Natl Acad Sci USA*. 2020;117: 6901–6909. pmid:32165537
[View Article](#) • [PubMed/NCBI](#) • [Google Scholar](#)

38. Ezer D, Jung J-H, Lan H, Biswas S, Gregoire L, Box MS, et al. The evening complex coordinates environmental and endogenous signals. *Nature Plants*. 2017; 1–12. pmid:28650433
[View Article](#) • [PubMed/NCBI](#) • [Google Scholar](#)

39. Mizuno N, Kinoshita M, Kinoshita S, Nishida H, Fujita M, Kato K, et al. Loss-of-Function Mutations in Three Homoeologous *PHYTOCHROME* Genes in Common Wheat Are Associated with the Extra-Early Flowering Phenotype. *PLoS ONE*. 2016;11: e0165618. pmid:27788250
[View Article](#) • [PubMed/NCBI](#) • [Google Scholar](#)

40. Andrade L, Lub Y, Cordeiro A, Costa JMF, Wigge PA, Saibo NJM, et al. The evening complex integrates photoperiod signals to control flowering. *Proc Natl Acad Sci USA*. 2022;119:e2122582119. pmid:35733265
[View Article](#) • [PubMed/NCBI](#) • [Google Scholar](#)

41. Yan L, Fu D, Li C, Blechl A, Tranquilli G, Bonafede M, et al. The wheat and barley vernalization gene *VRN3* is an orthologue of *FT*. Proc USA. 2006;103: 19581–19586. pmid:17158798
[View Article](#) • [PubMed/NCBI](#) • [Google Scholar](#)

42. Valverde F. CONSTANS and the evolutionary origin of photoperiodic timing of flowering. Journal of Experimental Botany. 2011;62: 2453–2463. pmid:21239381
[View Article](#) • [PubMed/NCBI](#) • [Google Scholar](#)

43. Pearce S, Shaw LM, Lin H, Cotter JD, Li C, Dubcovsky J. Night-break experiments shed light on the *Photoperiod 1*-mediated flowering pathway in *Brachypodium distachyon*. Nature Communications. 2017; pp.00361.2017–45. pmid:28408541
[View Article](#) • [PubMed/NCBI](#) • [Google Scholar](#)

44. Qin Z, Bai Y, Muhammad S, Wu X, Deng P, Wu J, et al. Divergent roles of *FT-like 9* in flowering transition under different day lengths in *Brachypodium distachyon*. Nature Communications. 2019;10: 1–10. pmid:30778068
[View Article](#) • [PubMed/NCBI](#) • [Google Scholar](#)

45. Yan L, Loukoianov A, Tranquilli G, Helguera M, Fahima T, Dubcovsky J. Positional cloning of the wheat vernalization gene *VRN1*. Proc USA. 2003;100: 6263–6268. pmid:12730378
[View Article](#) • [PubMed/NCBI](#) • [Google Scholar](#)

46. Li C, Dubcovsky J. Wheat FT protein regulates *VRN1* transcription through interactions with FDL2. Plant J. 2008;55: 543–554. pmid:18330200
[View Article](#) • [PubMed/NCBI](#) • [Google Scholar](#)

47. Yan L, Loukoianov A, Blechl A, Tranquilli G, Ramakrishna W, San Miguel P, et al. The wheat *VRN2* gene is a flowering repressor downregulated by vernalization. Science. 2004;303: 1640–1644. pmid:15016992
[View Article](#) • [PubMed/NCBI](#) • [Google Scholar](#)

48. Distelfeld A, Dubcovsky J. Characterization of the maintained vegetative phase deletions from diploid wheat and their effect on *VRN2* and *VRN3* expression levels. Mol Genet Genomics. 2010;283: 223–232. pmid:20063107
[View Article](#) • [PubMed/NCBI](#) • [Google Scholar](#)

49. Ream TS, Woods DP, Schwartz CJ, Sanabria CP, Mahoy JA, Walters EM, et al. Interaction of Photoperiod and Vernalization Determinants in *Brachypodium distachyon*. Plant Physiol. 2014;164: 694–709. pmid:24357601
[View Article](#) • [PubMed/NCBI](#) • [Google Scholar](#)

50. Woods DP, McKeown MA, Dong Y, Preston JC, Amasino RM. Evolution of *VRN2/Ghd7-Like* Genes in Vernalization-Mediated Repressors of Flowering. Plant Physiol. 2016;170: 2124–2135. pmid:26848096
[View Article](#) • [PubMed/NCBI](#) • [Google Scholar](#)

51. Corbesier L, Vincent C, Jang S, Fornara F, Fan Q, Searle I, et al. FT Protein Movement Contributes to Long-Distance Signaling in *Arabidopsis*. Science. 2007;316: 1030–1033. pmid:17446353
[View Article](#) • [PubMed/NCBI](#) • [Google Scholar](#)

52. Tamaki S, Matsuo S, Wong HL, Yokoi S, Shimamoto K. Hd3a protein is a mobile flowering signal in rice. Science. 2007;316(5827):1033–1036. pmid:17446351
[View Article](#) • [PubMed/NCBI](#) • [Google Scholar](#)

53. Cheng M-C, Kathare PK, Paik I, Huq E. Phytochrome Signaling Networks. Annu Rev Plant Biol. 2021;72: 217–244. pmid:33756095
[View Article](#) • [PubMed/NCBI](#) • [Google Scholar](#)

54. Quail PH. Phytochrome Photosensory Signalling Networks. *Nat Rev Mol Cell Biol*. 2002;3: 85–93. pmid:11836510
[View Article](#) • [PubMed/NCBI](#) • [Google Scholar](#)

55. Möglich A, Yang X, Ayers RA, Moffat K. Structure and Function of Plant Photoreceptors. *Annu Rev Plant Biol*. 2010;61: 21–47. pmid:20000000
[View Article](#) • [PubMed/NCBI](#) • [Google Scholar](#)

56. Mathews S. Evolutionary Studies Illuminate the Structural-Functional Model of Plant Phytochromes. *Plant Cell*. 2010;22: 4–16. pmid:20000000
[View Article](#) • [PubMed/NCBI](#) • [Google Scholar](#)

57. Chen A, Li C, Hu W, Lau MY, Lin H, Rockwell NC, et al. *PHYTOCHROME C* plays a major role in the acceleration of wheat flowering under photoperiod. *Proc Natl Acad Sci USA*. 2014. pmid:24961368
[View Article](#) • [PubMed/NCBI](#) • [Google Scholar](#)

58. Woods DP, Ream TS, Minevich G, Hobert O, Amasino RM. *PHYTOCHROME C* is an essential light receptor for photoperiodic flowering in grass, *Brachypodium distachyon*. *Genetics*. 2014;198: 397–408. pmid:25023399
[View Article](#) • [PubMed/NCBI](#) • [Google Scholar](#)

59. Pearce S, Kippes N, Chen A, Debernardi JM, Dubcovsky J. RNA-seq studies using wheat *PHYTOCHROME B* and *PHYTOCHROME C* reveal shared and specific functions in the regulation of flowering and shade-avoidance pathways. *BMC Plant Biol*. *BMC Plant Biology*; 2016;16: 1–11. pmid:27329140
[View Article](#) • [PubMed/NCBI](#) • [Google Scholar](#)

60. Monte E, Alonso JM, Ecker JR, Zhang Y, Li X, Young J, et al. Isolation and characterization of *phyC* mutants in *Arabidopsis* reveals commonalities between phytochrome signaling pathways. *Plant Cell*. 2003;15: 1962–1980.
[View Article](#) • [Google Scholar](#)

61. Takano M, Inagaki N, Xie X, Yuzurihara N, Hihara F, Ishizuka T, et al. Distinct and cooperative functions of phytochromes A, B, and C in deetiolation and flowering in rice. *Plant Cell*. 2005;17: 3311–3325. pmid:16278346
[View Article](#) • [PubMed/NCBI](#) • [Google Scholar](#)

62. Kippes N, VanGessel C, Hamilton J, Akpinar A, Budak H, Dubcovsky J, et al. Effect of *phyB* and *phyC* loss-of-function mutations on the transcriptome under short and long day photoperiods. *BMC Plant Biology*; 2020: 1–17. pmid:32600268
[View Article](#) • [PubMed/NCBI](#) • [Google Scholar](#)

63. Liu XL, Covington MF, Fankhauser C, Chory J, Wagner DR. ELF3 encodes a circadian clock–regulated nuclear protein that functions in the *PHYB* signal transduction pathway. *Plant Cell*. 2001;13: 1293–1304. pmid:11402161
[View Article](#) • [PubMed/NCBI](#) • [Google Scholar](#)

64. Saito H, Ogiso-Tanaka E, Okumoto Y, Yoshitake Y, Izumi H, Yokoo T, et al. Ef7 encodes an ELF3-like protein and promotes rice flowering by regulating the floral repressor gene *Ghd7* under both short- and long-day conditions. *Plant and Cell Physiology*. 2012;53: 717–728. pmid:22620000
[View Article](#) • [PubMed/NCBI](#) • [Google Scholar](#)

65. Dalmais M, Antelme S, Ho-Yue-Kuang S, Wang Y, Darracq O, d'Yvoire MB, et al. A TILLING Platform for Functional Genomics in *Brachypodium distachyon*. *PLoS ONE*. 2013;8: e65503–10. pmid:23840336
[View Article](#) • [PubMed/NCBI](#) • [Google Scholar](#)

66. Alvarez A, Li C, Lin H, Joe A, Padilla M, Woods DP and Dubcovsky J. *EARLY FLOWERING 3* interactions with *PHYTOCHROME B* and *PHYTOCHROME C* are critical for the photoperiodic regulation of wheat heading time. *PLoS Genetics*. 2022
[View Article](#) • [Google Scholar](#)

67. Woods D, Dong Y, Bouché F, Bednarek R, Rowe M, Ream T, et al. A florigen paralog is required for short-day vernalization in a pooid grass. *Plant Physiol.* 2015;167: 187–193. pmid:30618375
[View Article](#) • [PubMed/NCBI](#) • [Google Scholar](#)

68. Nieto C, López-Salmerón V, Davière J-M, Prat S. ELF3-PIF4 Interaction Regulates Plant Growth Independently of the Evening Complex. *Plant Physiol.* 2015;167: 187–193. pmid:25557667
[View Article](#) • [PubMed/NCBI](#) • [Google Scholar](#)

69. Yeom M, Kim H, Lim J, SHIN A-Y, Hong S, KIM J-I, et al. How Do Phytochromes Transmit the Light Quality Information to the Circadian Clock in *Arabidopsis*? *Molecular Plant*. 2014;7: 1701–1704. pmid:25095795
[View Article](#) • [PubMed/NCBI](#) • [Google Scholar](#)

70. Murakami M, Tago Y, Yamashino T, Mizuno T. Comparative Overviews of Clock-Associated Genes of *Arabidopsis thaliana* and *Oryza sativa*. *Plant Physiol.* 2006;141: 110–121. pmid:17132630
[View Article](#) • [PubMed/NCBI](#) • [Google Scholar](#)

71. Zhao J, Huang X, Ouyang X, Chen W, Du A, Zhu L, et al. *OsELF3-1*, an Ortholog of *Arabidopsis* *EARLY FLOWERING 3*, Regulates Rhythmic and Photoperiodic Flowering. *PLoS ONE*. 2012;7: e43705. pmid:22912900
[View Article](#) • [PubMed/NCBI](#) • [Google Scholar](#)

72. Itoh H, Tanaka Y, Izawa T. Genetic Relationship Between Phytochromes and *OsELF3-1* Reveals the Mode of Regulation for the Suppression of Phytochrome Signaling in Rice. *Plant and Cell Physiology*. 2019;60: 549–561. pmid:30476313
[View Article](#) • [PubMed/NCBI](#) • [Google Scholar](#)

73. Ishikawa R, et al. *Phytochrome B* regulates *Heading date 1 (Hd1)*-mediated expression of rice florigen *Hd3a* and critical day length in rice. *Genomics*. 2011; 285:461–470. pmid:21512732
[View Article](#) • [PubMed/NCBI](#) • [Google Scholar](#)

74. Koo B-H, Yoo S-C, Park J-W, Kwon C-T, Lee B-D, An G, et al. Natural variation in *OsPRR37* regulates heading date and contributes to a wide range of latitudes. *Molecular Plant*. 2013;6: 1877–1888. pmid:23713079
[View Article](#) • [PubMed/NCBI](#) • [Google Scholar](#)

75. Murphy RL, Klein RR, Morishige DT, Brady JA, Rooney WL, Miller FR, et al. Coincident light and clock regulation of pseudoresponse regulator (PRR37) controls photoperiodic flowering in sorghum. *Proc Natl Acad Sci USA*. 2011;108: 16469–16474. pmid:21930910
[View Article](#) • [PubMed/NCBI](#) • [Google Scholar](#)

76. Woods DP, Ream TS, Bouché F, Lee J, Thrower N, Wilkerson C, et al. Establishment of a vernalization requirement in *Brachypodium distachyon* by *REPRESSOR OF VERNALIZATION1*. *Proc Natl Acad Sci USA*. 2017;114: 6623–6628. pmid:28584114
[View Article](#) • [PubMed/NCBI](#) • [Google Scholar](#)

77. Dubcovsky J, Loukoianov A, Fu D, Valarik M, Sanchez A, Yan L. Effect of Photoperiod on the Regulation of Wheat Vernalization Genes. *Plant Mol Biol.* 2006;60: 469–480. pmid:16525885
[View Article](#) • [PubMed/NCBI](#) • [Google Scholar](#)

78. Gawronski P, Ariyadasa R, Himmelbach A, Poursarebani N, Kilian B, Stein N, et al. A distorted circadian clock causes early flowering and dependent variation in spike development in the *Eps-3A^m* mutant of einkorn wheat. *Genetics*. 2014;196(4):1253–1266. pmid:24443443
[View Article](#) • [PubMed/NCBI](#) • [Google Scholar](#)

79. De Mendiburu R-project org package agricolae accessed 25 July F, 2012. *Agricolae: Statistical procedures for agricultural research*. R 1.1–3. Comprehensive R Arch.